

UNDERSTANDING TSUNAMI RISK TO STRUCTURES: A CANADIAN PERSPECTIVE

D. Palermo¹ and I. Nistor¹

¹ *Assistant Professor, Dept. of Civil Engineering , University of Ottawa, Ottawa, Canada
Email: palermo@eng.uottawa.ca, inistor@uottawa.ca*

ABSTRACT

The potential catastrophic effects of tsunami-induced loading on built infrastructure in the vicinity of shorelines have been brought to the fore by recent global events. However, state-of-the-art building codes remain silent or provide conflicting guidance on designing near-shoreline structures in tsunami-prone areas. This paper focuses on tsunami-induced loading and its effect on structures within the Canadian context. The mechanics of tsunami-induced loading is described based on knowledge gained during reconnaissance visits after the 2004 south-east Asia Tsunami, as well as post-construction visits to countries significantly affected by the destructive forces of the tsunami. To gain an appreciation of the magnitude of tsunami-induced bores for a given seismic event along the western coastal region of Canada, structural analysis of a simple near-shoreline structure was performed considering a proposed loading protocol for tsunami-induced hydraulic bores. These loads were further compared to seismic loading in order to provide an estimation of the tsunami risk and its impact. The work was complemented by experimental results from a large-scale testing program conducted with the purpose of estimating the forces experienced on structural components. Square-, rectangular-, and diamond-shaped columns were used to study the influence of shape. Furthermore, results from debris impact testing are also discussed.

KEYWORDS: Tsunami, structures, hydrodynamics, surge, debris impact, loading combinations

1. INTRODUCTION

As awareness of the significant threat of tsunami loading on coastal and near coastal structures increases, so too does the need for guidance for engineers involved in designing structures located near coastlines, in high risk tsunami-prone areas. The National Building Code of Canada (NBCC 2005) does not provide, for the most part, guidelines for the design for tsunami-induced effects. Commentary J, "Design for Seismic Effects," states that damage to buildings as a result of an earthquake can arise from ground shaking, soil failures, surface fault ruptures, or tsunamis. However, only ground shaking and soil conditions are explicitly considered. The commentary indicates that other hazards can be addressed through planning and site selection. This may lead structural engineers to assume that tsunamis are not critical and would not generate a significant loading event on structures.

2. CANADIAN TSUNAMI HAZARD

Given its geographical location and its proximity to highly active seismic areas, Canada remains susceptible to tsunamis, particularly along the west coast, where British Columbia meets the Pacific Ocean. Table 1 provides a list of major historical tsunami events that have affected the western coastlines of North America.

Table 1 Historical Tsunami Events along Canada's Coastlines

Date	Location	Maximum Run-up (m)
Nov. 4, 1994	Southern Alaska	7.6
Feb. 4 1965	Western Alaska	10.7
Mar. 28, 1964	Gulf of Alaska	67.1
Mar. 9, 1957	Central Alaska	22.8
June 23, 1946	British Columbia	30
Sept. 10 1899	Gulf of Alaska	60
Nov. 18, 1929	Grand Banks, Newfoundland	13
Jan. 26, 1700	Cascadia, British Columbia	

Several of the events in Table 1 indicate that the tsunami hazard for Canada is significant, particularly for the Pacific coast. The March 28, 1964 Tsunami, which was triggered by a large earthquake in Alaska, resulted in millions of dollars in damage in Port Alberni, British Columbia. On January 26, 1700 a thrust fault rupture along the Cascadia Fault generated an earthquake measuring 9.0 on the Richter scale. This event triggered a tsunami wave that crossed the Pacific Ocean. According to oral traditions of First Nations, the tsunami completely destroyed the village of Pachena Bay situated on the west coast of Vancouver Island. There were no survivors. Given the presence of the Cascadia Fault and the Pacific "Rim of Fire", western Canada remains susceptible to tsunami events. To a lesser extent, the east coast of Canada, which borders the Atlantic Ocean, can also be affected, though not as often as the west coast, by tsunamis. On November 18, 1929, a 7.2 magnitude earthquake struck approximately 250 km south of Newfoundland, along the

southern edge of the Grand Banks, causing a large submarine landslide. In turn, a tsunami was generated, which hit the Burin Peninsula of Newfoundland, claiming 29 lives. This event represents the largest documented human loss in Canada linked to an earthquake. Note though, the tsunami was entirely responsible for the fatalities.

To understand the threat to western Canada, it is important to understand the geological features off the coast of British Columbia. From northern Vancouver Island to northern California, the Cascadia subduction zone marks the boundary between the smaller offshore Juan de Fuca Plate that is sliding under the much larger North American Plate. The Cascadia subduction zone has the potential to generate very large earthquakes, with magnitude 9.0 or greater, if the fault ruptures over its entire area. The January 26, 1700, Cascadia earthquake produced a fault rupture with a length of 1000 km. This type of event is similar to the 2004 Indian Ocean Earthquake, were the fault ruptured along an estimated length of 1300 km. Interestingly, both subduction zones run predominantly in a north-south direction, thus having the potential to trigger major tsunamis in the east-west direction. For Cascadia, this means that tsunami waves would propagate towards Vancouver Island. Popular belief suggests that major nearby cities, including Vancouver, Victoria, Seattle, and Portland, which are located on inland waterways rather than on the coast, would be sheltered from the full brunt of a tsunami wave. Meanwhile, numerical modeling has shown that tsunami waves would travel around Vancouver Island through diffraction and impact Victoria and Vancouver significantly (Xie *et al.*, 2007). This is consistent with observations following the 2004 Indian Ocean Tsunami, particularly on the west coast of Sri Lanka which was devastated by the tsunami as a result of wave propagation and diffraction around the island. Therefore, a megathrust earthquake along the Cascadia subduction zone has the potential to generate a major tsunami which would travel into the Juan de Fuca Strait, affecting communities along its shores.

Understanding the tsunami hazard is a major challenge in the design of near-shoreline structures. However, hazard maps, which would provide inundation depths and velocities for design in the case of a tsunami with a given magnitude and a given return period, are currently not available. At present, numerical modeling is employed to provide expected inundation depths for a given earthquake. Xie *et al.* (2007) conducted numerical modeling of tsunamis generated from a Cascadia Fault earthquake to assess the potential tsunami risk for western Canada. A magnitude 9.0 earthquake, similar to the event of 1700, was assumed in their model. The numerical model TSUNAMI N2 was employed. The model estimated a maximum wave run-up of 25 m along the western shore of Vancouver Island, with an estimated arrival time for the first wave of 1 hour and 20 minutes.

3. DESIGN CODES

Design codes in North America, which specifically address tsunami loading, are scarce. The City and County of Honolulu Building Code (CCH, 2000) and the Federal Emergency Management Agency Coastal Construction Manual (FEMA 55, 2003) are two documents that provide some guidance to engineers. The forces explicitly cited for a tsunami event

include buoyant forces, hydrostatic forces, hydrodynamic forces, debris impact forces, and surge or wave breaking forces. There are significant differences between the two documents. CCH determines surge forces generated by a tsunami bore-type wave, specifically for wall-type structural components. FEMA, on the other hand, considers wave breaking, which is typical of coastal floods and storm events. The FEMA document does not specifically address tsunami bores, which possess characteristics similar to those experienced during the December 24, 2004 Indian Ocean Tsunami. The other significant difference lies in the estimation of the flow velocity used in estimating the drag force. In CCH, the bore velocity is estimated to equal the depth of water at the building. FEMA, on the other hand, provides a significantly higher velocity in the area near the shoreline during a tsunami event. The flow velocity is estimated as $2\sqrt{gd_s}$, where d_s is the design flood depth. The consequence is larger drag forces in comparison to the estimates given by CCH. Only FEMA provides load combinations for the given force components; however, these combinations are explicitly formulated for flood scenarios and include wave breaking forces. Nistor *et al.* (2008) proposed loading combinations (Figure 1) that specifically consider a tsunami event including the effects of a bore-type wave.

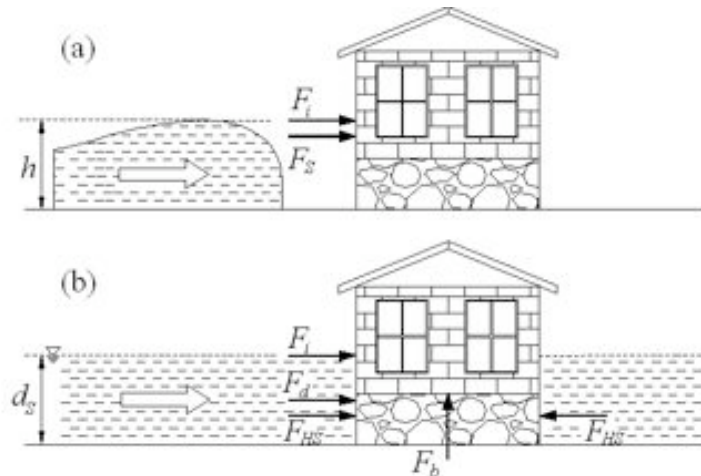


Figure 1 Proposed Tsunami Loading Combinations: a) Initial Impact; b) Post Impact (Nistor *et al.* 2008)

The first loading combination (Initial Impact) considers surge and debris impact forces as the main lateral load components. This represents the first impact of the tsunami bore. The second scenario (Post Impact) includes debris impact, hydrodynamic, and hydrostatic forces as the lateral loads. Note that the net hydrostatic forces typically provide an insignificant lateral load to the structure as a whole. However, the hydrostatic force may be more important in the evaluation of loads on an individual wall element. In addition to the lateral loads, a buoyant force component is included in the post impact event. This force can cause stability problems, including a reduction in the sliding and overturning resistance of a structure. Furthermore, consideration should be given to the rapid rising water level within a structure that has been flooded. This phenomenon can result in significant uplift forces on flooring elements (Ghobarah *et al.*, 2006).

The tsunami load can be combined with other loads and implemented in building codes. From the National Building Code of Canada (NBCC 2005) perspective, load cases following the philosophy of earthquake loading are suggested as a preliminary framework. A tsunami load is considered to be an extreme event leading to the following three load cases (Eqn. 1.1). The first load case considers Tsunami (T) and Dead (D) loads only. The second load case includes companion loads, including Live (L) and Snow (S) loads. The third case should only be considered if early warning systems provide sufficient warning to allow occupants to exit buildings safely.

$$\begin{aligned}
 &1.0T + 1.0D \\
 &1.0T + 1.0D + 0.5L + 0.25S \\
 &1.0T + 1.0D + 0.25S
 \end{aligned}
 \tag{1.1}$$

Note that in the case of the Cascadia subduction zone along the western coastline of British Columbia, damage to structures may initial occur due to the triggering earthquake before the tsunami-induced loading arrives. In such cases, engineers should consider the effects of the tsunami load on softened or damaged structures.

4. STRUCTURAL ANALYSIS

A simple, 10-storey ductile reinforced concrete moment resisting frame structure is analyzed for tsunami and seismic loads for the Vancouver area. The tsunami inundation level is assumed to be 5 m. The seismic weight is approximately 4400 kN per floor and the storey heights are 3.65 m. Figure 2 shows a plan view of the structure, while Table 2 provides the force components considered in calculating the tsunami loading.

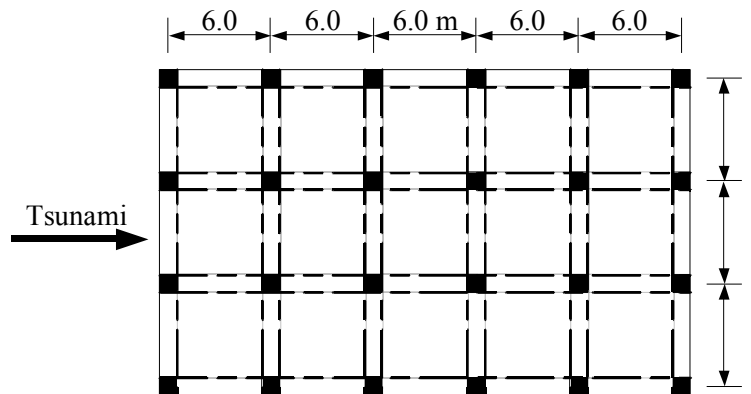


Figure 2 Building Plan Layout (Palermo *et al.*, 2007)

Table 2. Force Components for Tsunami Loading

Flow Velocity u	Surge F_S	Hydrodynamic F_d	Debris Impact F_i
$2\sqrt{gd_s}$	$4.5\rho gh^2b$	$\frac{\rho C_D Au^2}{2}$	$m \frac{u}{\Delta t}$

The calculated elastic base shear for the building under seismic effects is approximately 13720 kN, and considering ductility is 2020 kN. A 5 m tsunami level would induce an approximate base shear of 20360 kN due to the surge force during the initial impact and 11300 kN during the post impact caused by the drag of the tsunami flow around the structure. If the velocity component is assumed to be equal to the tsunami inundation level as assumed by CCH, the post impact phase would generate a base shear of 1730 kN. While this example is intended to provide an understanding of the tsunami forces imposed on structures, it also highlights the importance of properly quantifying the tsunami force components. The surge force is estimated as nine times the hydrostatic force; however, this has not been widely accepted in the literature. Furthermore, the velocity generated by the tsunami bore varies significantly, which affects the magnitude of the drag forces. This example also assumes that all non-structural exterior elements remain intact. It is highly probable that the first impact of the tsunami wave damages the exterior non-structural components, reducing the lateral load that is transferred to the structure. As such, the non-structural components act as a fuse for the lateral load resisting system. [Note: The debris impact loading according to FEMA and CCH is negligible in the calculation of the global base shear and has therefore been omitted.]

5. EXPERIMENTAL PROGRAM

Considerable disagreement and uncertainty exists in the literature regarding the force components and the tsunami-induced bore velocity. Particularly, the surge force is of question. To address and better understand the forces generated during a tsunami event, an exhaustive and comprehensive experimental program was conducted by the University of Ottawa in cooperation with the Canadian Hydraulics Centre in Ottawa, Canada.

The testing was carried out in a high discharge flume measuring 10.0 m in length, 2.7 m in width, and 1.4 m in height. The flume is serviced by pumps that can deliver a variable discharge flow up to 1.7 m³/s. For this experimental program, the flume was partitioned to create a testing zone 1.3 m wide and 7.3 m long. A hinged gate was designed and installed near the upstream section of the flume. In the closed position, the gate could impound a specified depth of water (impoundment depth). The hinging mechanism of the gate permitted a rapid opening, allowing a turbulent hydraulic bore to travel down the flume. Figure 3 provides a schematic of the testing facility.

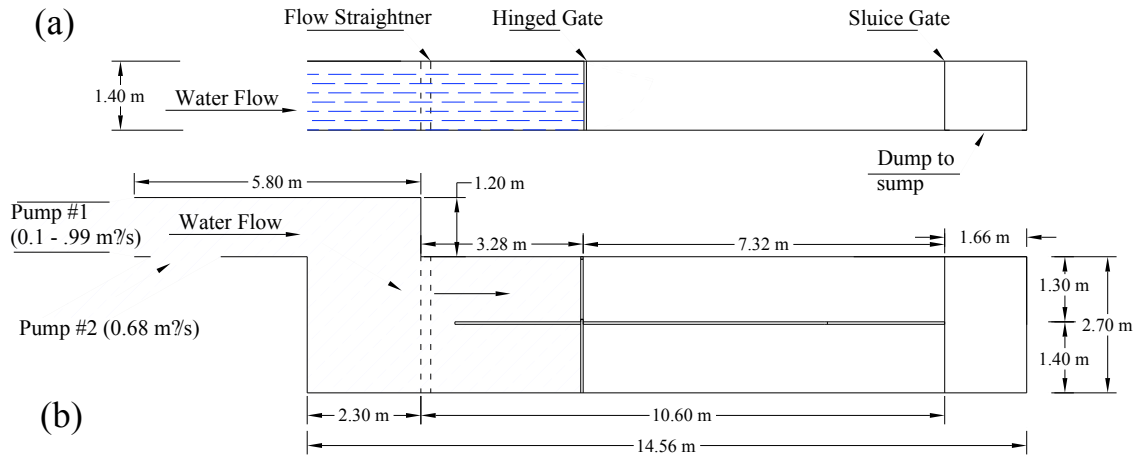


Figure 3 Wave Flume Setup: a) Elevation View; b) Plan View (Nouri 2008)

Forces created by the hydraulic bore were measured for two structural components: square/diamond, and circular sections. Figure 4 is a photo of the structural elements used for the experimental program of this study. The circular section was made of PVC pipe and measured 0.32 m in diameter, whereas the square/diamond section was assembled from acrylic Plexiglas and had a cross section of 0.2 m x 0.2 m. The circular section was mounted onto a 6-axis dynamometer, allowing base shears and moments to be recorded directly. In addition, nine pressure transducers were placed flush along a vertical column on the circular section. This was used to establish the time-history pressure profiles of the loading. The square/diamond section, on the other hand, was instrumented with five pressure transducers, which recorded local forces. The flume was equipped with ADV sensors and wave gauges to record flow velocities and depths, respectively.

The testing program consisted of 11 test series, and included varying upstream impoundment depths, debris weights, and constrictions. Additional information on the testing program is available in Nouri (2008). For brevity, a sample of the experimental testing will be discussed herein.



Figure 4 Circular and Square/Diamond Structural Components

6. EXPERIMENTAL RESULTS

Of particular interest to structural engineers are the force components expected during a tsunami event. Figure 5 provides the global force-time histories of the base shears experienced by the circular section.

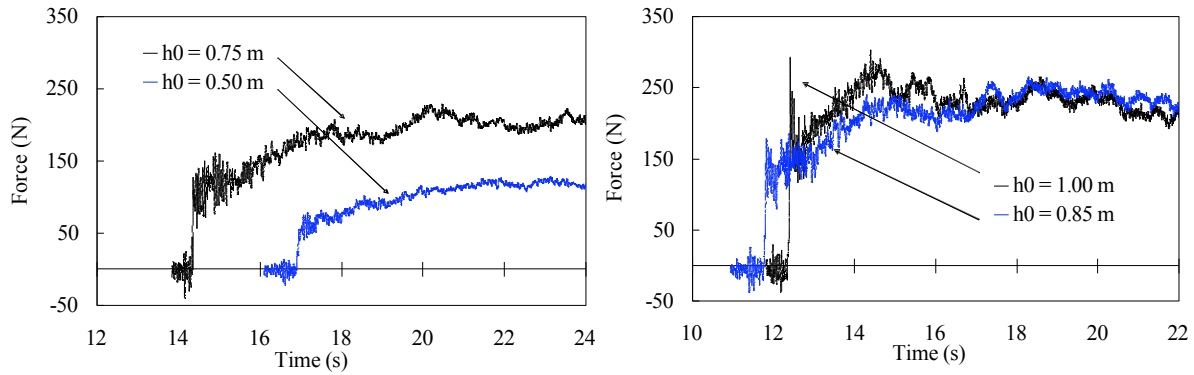


Figure 5 Force-Time History for Circular Section (Nouri 2008)

Figure 5 provides the base shears for impoundment depths of 0.5 m, 0.75 m, 0.85 m, and 1.0 m. The first abrupt rise in force is caused by the initial impact (surge force) of the hydraulic bore on the structure. With increasing upstream water depth, the surge force increases. This increase is partly due to the larger impoundment depth and the increase in bore front slope with increasing impoundment depth. Immediately following the initial impact, there is a drop in the base shear. For the 0.75 m, 0.85 m, and 1.0 m impoundment depths, the reduction in force ranges between 55% and 60% of the initial impacting force. For the 0.50 m impoundment depth, the drop in the base shear force is approximately 30% of the initial magnitude. This drop is followed by a gradual increase caused by the run-up of the hydraulic bore. In all cases, the run-up force was equal to or greater than the initial impacting load. The run-up is followed by a semi-steady state of flow characterizing the drag force. Excluding the 1.0 m impoundment depth, the drag force represented the largest force component in the loading history. Figure 6 shows the individual force components for a 1.0 m impoundment depth, along with the corresponding bore height.

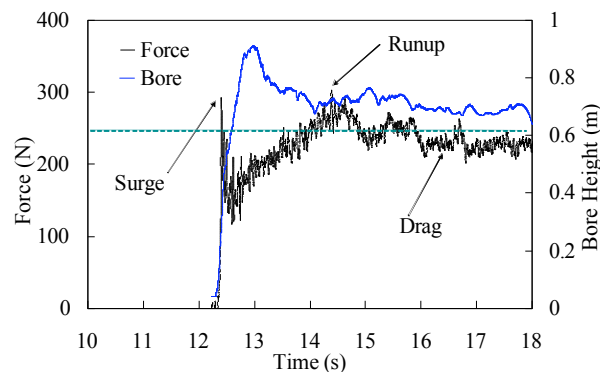


Figure 6 Time-History of Force Components on Circular Section

Figure 7 (a) provides the pressure-time history for the circular section along the height while Figure 7 (b) provides the pressure distribution corresponding to the individual force components.

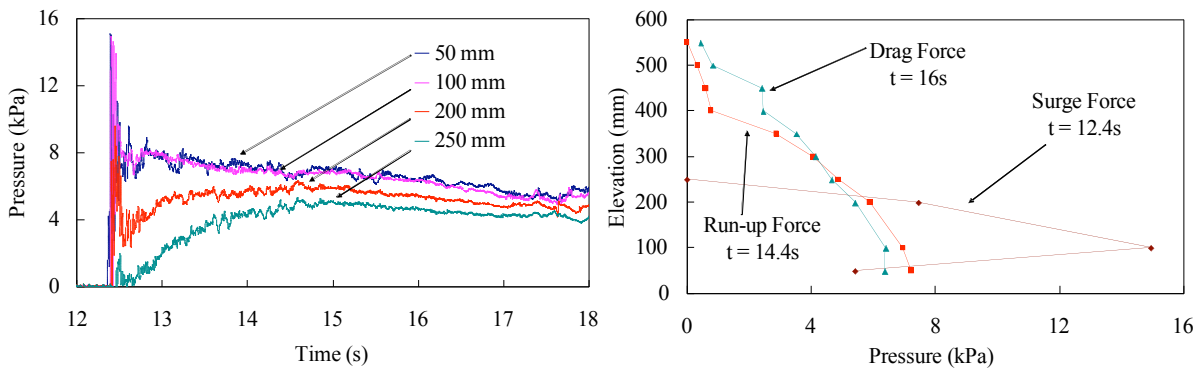


Figure 7 Pressures: a) Time-History Along Height of Column; b) Distribution Corresponding to Forces

Pressures are shown at 50 mm, 100 mm, 200 mm, and 250 mm from the base of the circular section. At the instant of the initial impact of the hydraulic bore, the pressure distribution is approximately triangular, as indicated by the surge force component at 12.4 s. The pressure distributions become increasingly constant at the point of the run-up and drag force components, shown at 14.4 s and 16 s, respectively. Variations in the velocity along the height of the bore are partly responsible for variations in pressure for the drag force component.

To simulate debris impact loading, a wooden log, 445 mm long and with a 90 mm x 90 mm cross-section, was used. Figure 8 illustrates the effect of debris on the force-time history for the circular section with impoundment depths of 1.0 m and 0.75 m. The debris caused a significant increase in the base shear recorded by the dynamometer mounted at the base of the circular section. A spike is evident a short time after the initial impact of the hydraulic bore. For the 1.0 m impoundment depth, an increase in the base shear force of 695 N occurred over a rise time of 0.0075 s, whereas the base shear force increased by 430 N over a period of 0.008 s for the 0.75 m impoundment. The results shown for the 0.75 m impoundment demonstrate a second peak a short time after the initial debris impact. This phenomenon was caused by a “bounce back” effect of the wooden log causing a subsequent impact. The second peak was always smaller in magnitude; however, the rise time was similar to the first debris impact. This “bounce back” effect was observed for other impoundment depths as well.

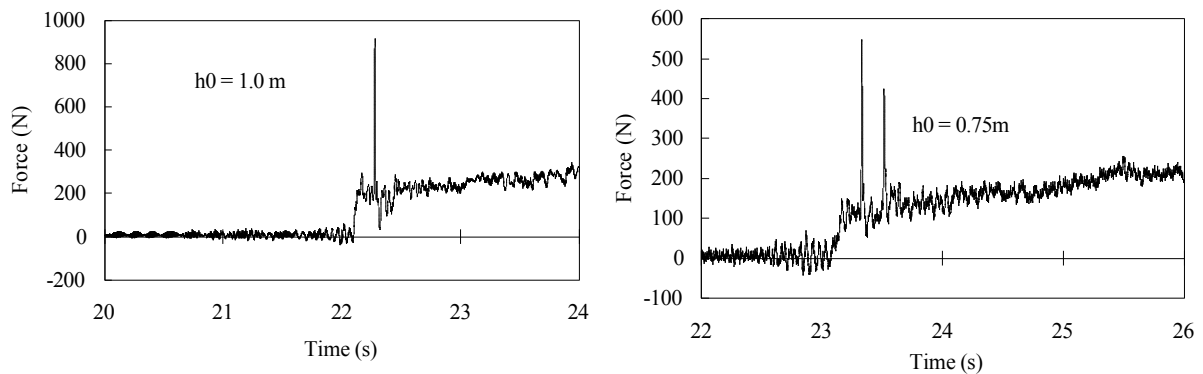


Figure 8 Debris Impact Loading on Circular Section

7. CONCLUSIONS

This paper provides background information regarding the tsunami threat to Canada and, in particular, the west coast. In addition, results from an experimental program, aimed at better understanding the forces generated by a turbulent hydraulic bore, are presented. The following conclusions are drawn from these experiences:

1. Tsunami-induced loading should be considered for near-shoreline structures located in tsunami-prone areas.
2. More guidance is required for structural engineers in order to estimate tsunami loads on structures.
3. Improved estimates of bore velocities are required to provide more accurate drag and debris impact forces.
4. Based on the impoundment depths investigated, the experimental results indicate that the surge force does not significantly overshoot the drag force as indicated by current codes.
5. Pressure readings of the circular section indicate that the initial bore impact causes an approximate triangular pressure distribution along the height of the section.
6. Debris impacting structures can produce a “bounce back” effect, causing a second lower amplitude impact.

REFERENCES

Canadian Commission on Building and Fire Codes (2005). "National Building Code of Canada (NBCC)," National Research Council of Canada, Ottawa, Canada.

Department of Planning and Permitting of Honolulu Hawaii (2000). "City and County of Honolulu Building Code," Chapter 16, Article 11.

Federal Emergency Management Agency (2003). "Coastal Construction Manual," FEMA 55, Jessup, MD.

Ghobarah, A., Saatcioglu, M. and Nistor, I., (2006). The impact of 26 December 2004 earthquake and tsunami on structures and infrastructure, *J. Engineering Structures*, Elsevier, Vol. 28, 312-326.

Nistor, I., Palermo, D. Nouri, Y., Murty, T., and Saatcioglu, M. (2008), Tsunami forces on structures, Chapter 11 in "*Handbook of Coastal and Ocean Engineering*", Editors: Dr. Kim Young (UCLA), World Scientific, Singapore (in press).

Nouri, Y. (2008). "The Impact of Hydraulic Bores and Debris on Free Standing Structures," M.A.Sc. Thesis, Department of Civil Engineering, University of Ottawa, Ottawa, Canada.

Palermo, D., Nistor, I., Nouri, Y., and Cornett, A. (2007). "Tsunami-Induced Impact and Hydrodynamic Loading of Near-Shoreline Structures." *PROTECT 2007* (First International Workshop of Performance, Protection, and Strengthening of Structures under Extreme Loading), Whistler, Canada.

Xie, J., Nistor, I., and Murty, T. (2007). "Tsunami Risk for Western Canada and Numerical Modeling of the Cascadia Fault Tsunami," *18th Canadian Hydrotechnical Conference*, Winnipeg, Canada.